Coupling Atomistic and Continuum Descriptions Using Dynamic Control

E.M. Kotsalis[1], J.H. Walther[1,2], P. Koumoutsakos[1]

[1] Computational Science and Engineering Laboratory, ETH Zurich, 8092, Zurich, Switzerland.
[2] Dept. of Mech. Engng., Technical University of Denmark, 2800 Lyngby, Denmark. petros@ethz.ch

Summary. We propose control algorithms to enhance the efficiency of a hybrid model coupling continuum and atomistic descriptions of dense liquids. Time and length scales are decoupled by using an iterative Schwarz domain decomposition algorithm. In this algorithm, the lack of periodic boundary conditions in the MD simulations leads to spurious density fluctuations at the continuum-atomistic interface. We remedy this problem by using an external boundary force determined by a simple control algorithm that acts to cancel the density fluctuations. The conceptual and algorithmic simplicity of the method makes it suitable for any type of coupling between atomistic, mesoscopic and continuum descriptions of dense liquids.

1 Introduction

The modeling and simulation of systems such as biosensors embedded in aqueous environments [1–4], microfluidic channels with nanopatterned walls or bluff bodies with superhydrophobic surfaces [5], requires a multiscale approach. Hybrid computations have been proposed in order to couple effectively atomistic and continuum descriptions for dense fluids. The atomistic effects are modeled using Molecular Dynamics (MD) while macroscale phenomena are described by the discretized, incompressible Navier-Stokes equations. Hybrid techniques can be -distinguished on the way information is exchanged between the two descriptions. In flux exchange schemes [6–9] the two descriptions communicate at an interface requiring a conservative exchange of fluid properties, while Schwartz domain decompositions [10–12] require an overlap region where the atomistic and continuum descriptions coevolve. In both algorithms, a critical issue is the elimination of periodicity from the MD system that is often associated with the appearance of density disturbances close to the boundary. Repulsive wall potentials [6, 7] and buffer regions [8, 9, 11] have been proposed in order to circumvent this difficulty. Werder et al. [12] combined a hard wall with boundary potentials based on the radial distribution

M. Ellero et al. (eds.), *IUTAM Symposium on Advances in Micro- and Nanofluidics*, IUTAM Bookseries 15,

function of the system that is being simulated in order to impose the local system pressure. This scheme was found to significantly reduce the density perturbations in the molecular system compared to existing algorithms and has been used in [13] to conduct multiscale simulations of a Lennard-Jones fluid flowing past and along the axis of a carbon nanotube, coupling MD to Lattice Boltzmann models. Here we employ a control algorithm [14] to adjust the boundary force in order to eliminate the oscillations in the density when exchanging information between atomistic and continuum domains.

2 Methodology

The atomistic region is described by MD simulations subject to non-periodic boundary conditions (NPBC). The position $\mathbf{r}_i = (x_i, y_i, z_i)$ and velocities $\mathbf{v}_i = (u_i, v_i, w_i)$ of the i-th particle evolve according to Newton's equation of motion:

$$\frac{d}{dt}\mathbf{r}_i = \mathbf{v}_i(t),$$
$$m_i \frac{d}{dt}\mathbf{v}_i = \mathbf{F}_i = -\sum_{j \neq i} \nabla U(r_{ij}),$$

where m_i is the mass and $\mathbf{F}_i$ the force on particle i. The interaction potential $U(r_{ij})$ models the physics of the system. Here we consider the monoatomic fluid of argon. Thus:

$$U(r_{ij}) = U_{12-6}(r_{ij}) + U_m(r_w; \rho, T),$$

where U_{12-6} is the 12–6 Lennard-Jones (LJ) potential:

$$U_{12-6}(r_{ij}) = 4\epsilon \left[\left(\frac{\sigma}{r_{ij}} \right)^{12} - \left(\frac{\sigma}{r_{ij}} \right)^{6} \right], \tag{1}$$

and r_{ij} denotes the distance between the i and j atom, and σ and ϵ are the length and energy scale of the LJ potential (for argon $\epsilon = 0.996$ kJ mol^{-1} and $\sigma = 0.340$ nm). The term $U_m(r_w; \rho, T)$ accounts for the interaction of the atomistic region with the surrounding medium. It depends on the distance to the outer boundary of the atomistic domain r_w, the local density ρ, and the local temperature T of the fluid. All interaction potentials are truncated for distances beyond a cutoff radius (r_c) of 1.0 nm. We note that increasing the cutoff from 1 nm to 2 nm does not affect the quality of the results. The equations of motion are integrated using the leap-frog scheme with a time step of 10 fs. We perform the MD simulations at different state points of the fluid and report quantities in reduced units ($T^* = k_B T/\epsilon$, $\rho^* = \rho\sigma^3$, and $P^* = P\sigma^3\epsilon$). In hybrid algorithms, the elimination of periodic boundary conditions in the atomistic domain hinders the maintenance of a uniform

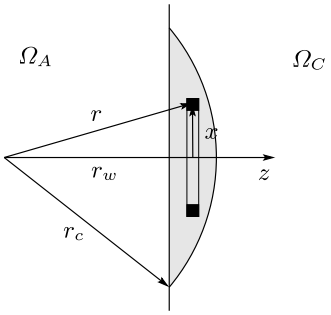

Fig. 1. Integration domains for the effective boundary force (2). The force contributions along z are integrated over the shaded area. The number of atoms in the infinitesimal ring element is $2\pi\rho_n g(r)xdxdz$, where ρ_n is the average number density and $g(r)$ the radial distribution function. Ω_A and Ω_C denote the atomistic and the continuum domains, respectively.

density across the domain and the proper calculation of the virial pressure. In order to correct for the "missing component" of the virial pressure, a boundary force is applied in the atomistic domain [6, 7, 11]. Hence, we impose NPBC in the x-direction with a wall force F_m to exert the correct mean virial pressure (P_U) on the MD system along with a specular wall to impose the ideal kinetic part (P_K) of the system pressure:

$$P = P_K + P_U = k_B T\rho_n + \rho_n \int_0^{r_c} F_m(r)dr,$$

where k_B is the Boltzmann constant. In [12] it was proposed to compute the wall force (F_m) from the pair potential (1) and the pair correlation function ($g(r)$) of the working fluid. This technique was shown to alleviate many of the drawbacks of existing methods and it constitutes the basis of the present algorithm. Thus the Lennard-Jones force of each particle weighted by $g(r)$ is integrated over the part of the cutoff sphere that lies outside of the atomistic domain, cf. Fig. 1,

$$F_m(r_w) = -2\pi\rho_n \int_{z=r_w}^{r_c} \int_{x=0}^{\sqrt{r_c^2-z^2}} g(r)\frac{\partial U_{12-6}(r)}{\partial r}\frac{z}{r}xdxdz. \qquad (2)$$

At the supercritical state point ($T^* = 1.8, \rho^* = 0.6$) [15] this approach was found to reduce drastically the spurious density fluctuations [12]. We examine the validity of this method in one additional state point in the liquid regime, namely ($T^* = 1.1, \rho^* = 0.81$). The size of the computational domain is 5 nm $\times$ 5 nm $\times$ 5 nm. The periodicity is broken in the x-direction. The system is weakly coupled to a Berendsen thermostat [16] with a time constant of 0.1 ps. After equilibration we heat only the atoms located in the cells close to the x boundary. For this new state point the method is found

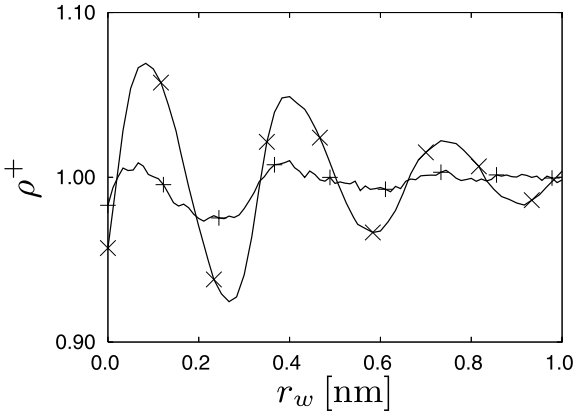

Fig. 2. The reduced density values ($\rho^+ = \rho/\rho_{bulk}$) of argon confined between hard walls and subject to the wall potential model of Werder et al. [12] up to a distance of a cutoff from the boundary. By reducing the temperature, while increasing the density, the amplitude of the oscillations becomes higher. —+— ($T^* = 1.8$, $\rho^* = 0.60$), —×— ($T^* = 1.1$, $\rho^* = 0.81$).

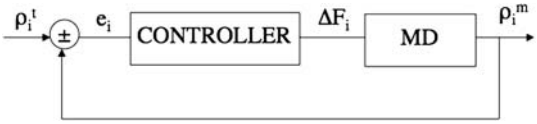

Fig. 3. Schematic of the control algorithm for reducing density fluctuations.

to encounter difficulties when lowering the temperature, while increasing the density, at constant pressure, leading to density oscillations close to the boundary (Fig. 2). The amplitude of these oscillations amounts to 8% and is well below previously reported values in hybrid simulations [12] but they may still cause unnecessary disturbances to the atomistic system. In order to eliminate the oscillations we apply a control algorithm for the mean external boundary force applied to the MD system. The control approach is sketched in Fig. 3. Each iteration involves the following steps: we start by applying the external boundary force as proposed in (2). Then we measure the density in short time intervals filtering away high frequency noise. The density $\rho^{m'}$ is measured with a spatial resolution δx of 0.0166 nm in time intervals of 30 ps and processed twice through a Gaussian filter resulting ρ^m as:

$$\rho^{m''}(x) = \frac{1}{\epsilon}\int \rho^{m'}(x)\exp\left(-\frac{(x-y)^2}{\epsilon^2}\right)dy,$$

$$\rho^{m}(x) = \frac{1}{\epsilon}\int \rho^{m''}(x)\exp\left(-\frac{(x-y)^2}{\epsilon^2}\right)dy,$$

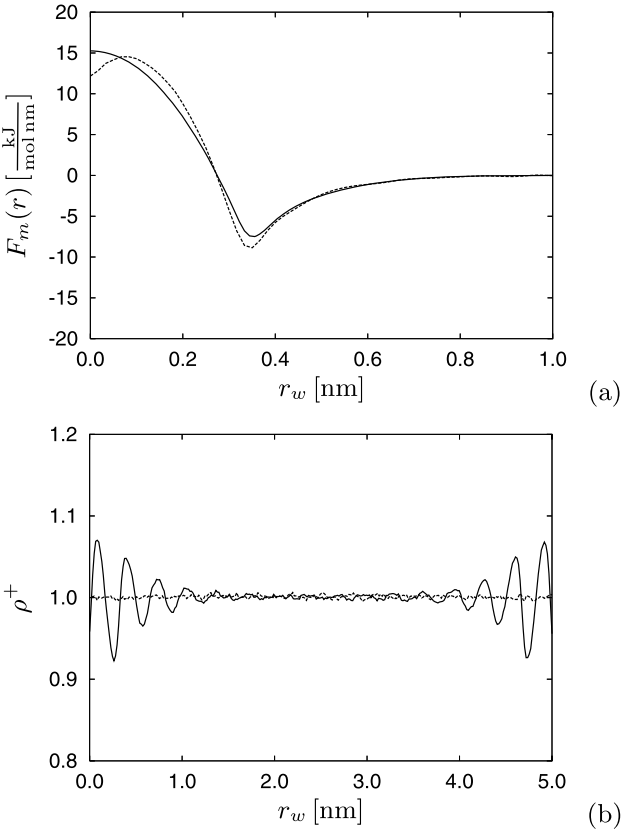

Fig. 4. (a) The initial external boundary force computed taking the fluid structure into account and the resulting one after applying the control algorithm at the state point ($T^* = 1.1, \rho^* = 0.81$). (b) The corresponding uncontrolled (—) and controlled reduced density values (- - -). The value used for K_P is 0.083 $\frac{\mathrm{nm}^3\,\mathrm{mol}}{\mathrm{amu\,kJ}}$ and both the force and density have been sampled over 10 ns.

where $\epsilon = 2\delta x$. The cutoff used for the discrete evaluation of the convolution is $3\delta x$. We then evaluate the error as:

$$e(r_w) = \rho^t - \rho^m(r_w), \tag{3}$$

where r_w is the distance to the boundary, ρ^t the desired constant target density and ρ^m the measured filtered value. We compute the gradient of this error as $\epsilon(r_w) = \nabla e(r_w) = -\nabla\rho^m(r_w)$ and amplify this with a factor K_P to obtain the changes ΔF in the boundary force as:

$$\Delta F_i = K_P \epsilon_i,$$

for each ith bin. The boundary force is finally computed as:

$$F_i^{new} = F_i^{old} + \Delta F_i,$$

After the root mean square (RMS) of the errors becomes less than a prescribed value, here 1%, we consider that the method has converged and we can start measuring the density for assessing the quality of the result. The controller online keeps acting on the system. We test this approach for the state point ($T^* = 1.1, \rho^* = 0.81$), where the mean force algorithm of Werder et al. [12] failed to fully eliminate the fluctuations. We set $K_P = 0.0830 \frac{\text{nm}^3\,\text{mol}}{\text{amu}\,\text{kJ}}$ and the results shown in Fig. 4 demonstrate that the method converges and eliminates the density oscillations. When compared with the initial force, we observe a decrease of the magnitude of the force close to the boundary and a shift for the location of the minimum. At larger distances from the wall ($r_w > 0.6$ nm) the shape of the force is not significantly altered. We find a value of $K_P = 0.0830 \frac{\text{nm}^3\,\text{mol}}{\text{amu}\,\text{kJ}}$ to guarantee good stability properties and fast convergence.

3 Couette Flow

Finally, we validate the control algorithm for the case of Couette flow of liquid argon ($T^* = 1.1, \rho^* = 0.81$) confined between two graphite surfaces. A sketch of the flow geometry is shown in Fig. 5. The size of the computational domain is 30.0 nm$\times$4.3 nm$\times$4.9 nm, small enough to allow a fully atomistic simulation which we will use as a reference. The number of computational boxes used for heating is $30 \times 1 \times 1$. The same resolution is used to sample the velocities that serve as a boundary condition (BC) for the continuum solver. The flow is imposed by moving the upper wall with a velocity $v = 100\ \text{m}\,\text{s}^{-1}$.

In the hybrid approach we apply the Schwarz alternating method with an overlap region of 4 cells (4 nm). Details about the exchange of boundary

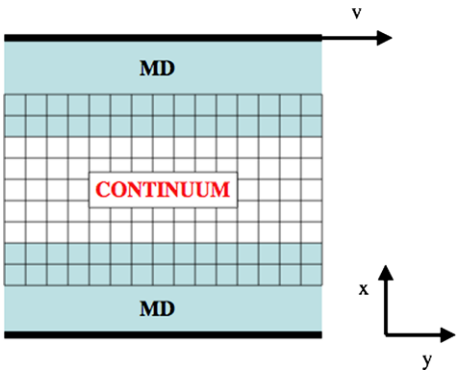

Fig. 5. Sketch of the hybrid simulation for the Couette flow. Shaded regions denote the domain of MD simulations and grid cells indicate simulations using the Navier-Stokes equations.

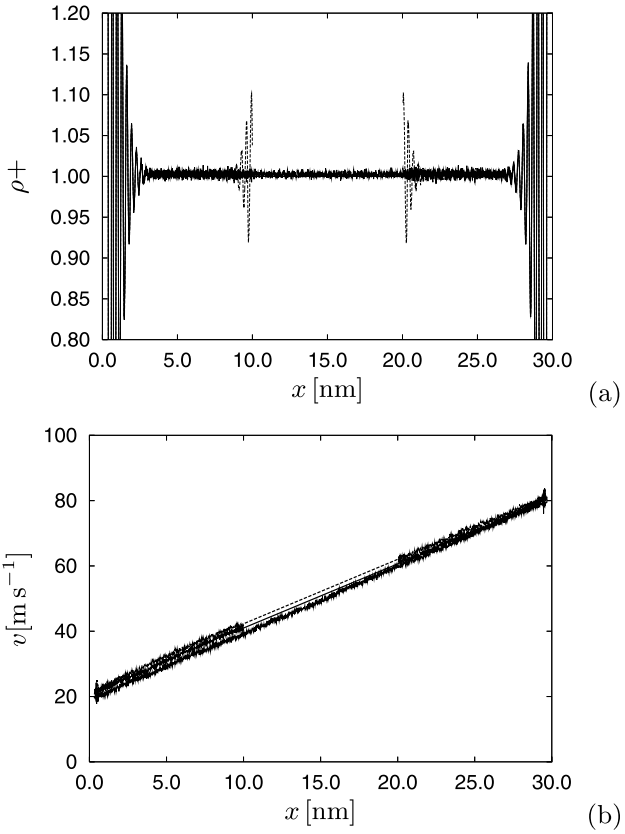

Fig. 6. (a) Reduced density profiles in the Couette flow of the reference MD simulations and of the hybrid controlled (—) and uncontrolled (– – –) cases. Density oscillations of the order of 10% in the uncontrolled case are eliminated by the controller. (b) Resulting velocity profiles in the Couette flow of the reference MD simulations and the hybrid controlled (—) and uncontrolled (– – –) cases.

conditions between the MD and the continuum region, described by incompressible Navier-Stokes (NS) equations, can be found in [12]. In the present case the solution to the NS equations is a linear streamwise velocity profile. In the hybrid approach the system contains a graphite surface and the argon atoms form layers in its vicinity. During equilibration we d Each MD subdomain in the hybrid case has the dimensions 10.0 nm × 4.3 nm × 4.9 nm (10 boxes in x and 1 box in y- and z-direction), large enough to resolve the extensive physical perturbations in the fluid density at the fluid-solid interface. In a cycle of the hybrid algorithm, we impose the boundary condition from the continuum to the MD, equilibrate the MD system for 20 ps to reach a new quasi-steady state and subsequently sample the velocities for 100 ps to extract the BC for the continuum. The flow reaches a steady state after

10 ns and we sample the results from 10 ns to 35 ns every 1 ps with a total of 25000 samples. In Fig. 6 we show the velocity and density profiles obtained from the hybrid simulations. We observe large physical perturbations in the density at the graphite surface and spurious oscillations at the continuum-MD interface in the uncontrolled case which are eliminated in the controlled one. The velocity profiles are similar in both cases.

4 Conclusions

We have presented a control algorithm to eliminate density fluctuations in the coupling of atomistic models with continuum descriptions of dense liquids using Schwarz domain decomposition. The algorithm is validated for fluids at rest and it is shown to eliminate density oscillations with amplitude of the order of 8%. Finally we demonstrated the capability of the algorithm for multiscale simulations by successfully coupling of MD simulations to a continuum description for the Couette flow problem.

References

1. Chen RJ, Bangsaruntip S, Drouvalakis KA, Kam NWS, Shim M, Li YM, Kim W, Utz PJ, Dai HJ (2003) Noncovalent functionalization of carbon nanotubes for highly specific electronic biosensors. Proc Natl Acad Sci USA 100(9):4984–4989
2. Li J, Ng HT, Cassell A, Fan W, Chen H, Ye Q, Koehne J, Han J, Meyyappan M (2003) Carbon nanotube nanoelectrode array for ultrasensitive DNA detection. Nano Lett 3(5):597–602
3. Lin Y, Taylor S, Li H, Shiral Fernando KA, Qu L, Wang W, Gu L, Zhou B, Sun Y (2004) Advances toward bioapplications of carbon nanotubes. J Mater Chem 14:527–541
4. Zheng M, Jagota A, Semke ED, Diner BA, McLean RS, Lustig SR, Richardson RE, Tassi NG (2003) DNA-assisted dispersion and separation of carbon nanotubes. Nat Matter 2:338–342
5. Watanabe K, Takayama T, Ogata S, Isozaki S (2003) Flow between two coaxial rotating cylinders with a highly water-repellent wall. AIChE J 49(8):1956–1963
6. O'Connell ST, Thompson PA (1995) Molecular dynamics-continuum hybrid computations: A tool for studying complex fluid flow. Phys Rev E 52(6):R5792–R5795
7. Flekkøy EG, Wagner G, Feder J (2000) Hybrid model for combined particle and continuum dynamics. Europhys Lett 52(3):271–276
8. Flekkoy E, Delgado-Buscalioni R, Coveney P (2005) Flux boundary conditions in particle simulations. Phys Rev E 72:026703
9. De Fabriitis G, Delgado-Buscalioni R, Coveney P (2006) Multiscale modeling of liquids with molecular specificity. Phys Rev Lett 97:134501
10. Hadjiconstantinou NG (1999) Hybrid atomistic-continuum formulations and the moving contact-line problem. J Comput Phys 154:245–265

11. Nie XB, Chen SY, E WN, Robbins MO (2004) A continuum and molecular dynamics hybrid method for micro- and nano-fluid flow. J Fluid Mech 500: 55–64
12. Werder T, Walther JH, Koumoutsakos P (2005) Hybrid atomistic-continuum method for the simulation of dense fluid flows. J Comput Phys 205:373–390
13. Dupuis A, Kotsalis E, Koumoutsakos P (2007) Coupling lattice Boltzmann and molecular dynamics models for dense fluids. Phys Rev E 75:046704
14. Kotsalis E, Walther J, Koumoutsakos P (2007) Control of density fluctuations in atomistic-continuum simulations of dense liquids. Phys Rev E 76:016709
15. Johnson JK, Zollweg JA, Gubbins KE (1993) The Lennard-Jones equation of state revisited. Mol Phys 78(3):591–618
16. Berendsen HJC, Postma JPM, van Gunsteren WF, DiNola A, Haak JR (1984) Molecular dynamics with coupling to an external bath. J Chem Phys 81(8):3684–3690